Functional copper at the acetyl-CoA synthase active site
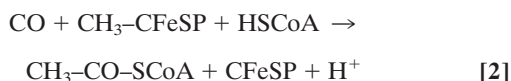
Javier Seravalli*, Weiwei Gu†, Annie Tam‡, Erick Strauss‡, Tadhg P. Begley‡, Stephen P. Cramer†, and Stephen W. Ragsdale*§

*Department of Biochemistry, University of Nebraska, Lincoln, NE 68588; ‡Department of Chemistry and Chemical Biology, Cornell University, Ithaca, NY 14853; and †Department of Applied Science, University of California, Davis, CA 95616

The bifunctional CO dehydrogenase/acetyl-CoA synthase (CODH/ACS) plays a central role in the Wood–Ljungdahl pathway of autotrophic CO_2 fixation. A recent structure of the *Moorella thermoacetica* enzyme revealed that the ACS active site contains a [4Fe-4S] cluster bridged to a binuclear Cu-Ni site. Here, biochemical and x-ray absorption spectroscopic (XAS) evidence is presented that the copper ion at the *M. thermoacetica* ACS active site is essential. Depletion of copper correlates with reduction in ACS activity and in intensity of the ''NiFeC'' EPR signal without affecting either the activity or the EPR spectroscopic properties associated with CODH. In contrast, Zn content is negatively correlated with ACS activity without any apparent relationship to CODH activity. Cu is also found in the methanogenic CODH/ACS from *Methanosarcina thermophila*. XAS studies are consistent with a distorted Cu(I)–S₃ site in the fully active enzyme in solution. Cu extended x-ray absorption fine structure analysis indicates an average Cu–S bond length of 2.25 Å and a metal neighbor at 2.65 Å, consistent with the Cu–Ni distance observed in the crystal structure. XAS experiments in the presence of seleno-CoA reveal a Cu–S₃Se environment with a 2.4-Å Se–Cu bond, strongly implicating a Cu–SCoA intermediate in the mechanism of acetyl-CoA synthesis. These results indicate an essential and functional role for copper in the CODH/ACS from acetogenic and methanogenic organisms.

T he bifunctional enzyme CO dehydrogenase/acetyl-CoA synthase (CODH/ACS; EC 1.2.99.2) plays a central role in the Wood–Ljungdahl pathway of autotrophic CO_2 fixation (1, 2). CODH catalyzes the two-electron reduction of CO_2 to CO (Eq. **1**). The CO is directed through a 70-Å channel to the ACS active site, where it is condensed with a methyl group (donated by the methylated corrinoid iron–sulfur protein, CH_3-CFeSP), and CoA to generate acetyl-CoA (Eq. **2**) (3).

$$CO_2 + 2 \text{ electrons} + 2 H^+ \rightarrow CO + H_2O \qquad [1]$$

$$CO + CH_3–CFeSP + HSCoA \rightarrow$$

$$CH_3–CO–SCoA + CFeSP + H^+ \qquad [2]$$

A recent crystal structure reveals that CODH/ACS is a 300-kDa $\alpha_2\beta_2$ protein with two core CODH β subunits tethered on each side to two ACS α subunits (4). The A cluster in each α subunit contains 1 Ni, 1 Cu, and 4 Fe ions, whereas the β subunit contains 1 Ni and 10 Fe ions arranged into three clusters, known as B, C, and D. Various studies indicate that Ni is a required component of CODH in acetogenic bacteria (5, 6) and *Rhodospirillum rubrum* (7). Ni also is essential for ACS activity, and a subpopulation of the Ni ions in the ACS active site, called the "labile Ni," is required for ACS activity and for generation of an EPR signal called the "NiFeC signal" (8). When CODH/ACS is reacted with CO, this EPR signal forms and, upon reaction with the CH_3–CFeSP, it decays, both reactions occurring at catalytically relevant rates, indicating intermediacy of the NiFeC species in

the ACS catalytic cycle (9). Until recently (4), Cu was not known to be a component of CODH/ACS. The discovery of Cu at the ACS active site was surprising, given that this enzyme has been studied for many years and this metal had never been previously reported in a CODH/ACS.¶ Cu was found in the *Methanosarcina barkeri* CODH (10); however, ACS was not present in this preparation of methanogenic enzyme, and Cu has not been reported in the three CODH crystal structures (4, 11, 12) or in other CODHs that have been characterized. A relationship between Cu content and ACS activity was indicated in an earlier report (4); here we provide convincing biochemical and spectroscopic evidence for the importance of Cu in the ACS mechanism.

Materials and Methods

Materials. CO (99.99%) and N_2 (99.998%) were purchased from Matheson Gas (Joliet, IL). N_2 (99.998%; Linde, Lincoln, NE) and other inert gases were purified of traces of oxygen by passage over a heated BASF catalyst (R3-11G). Titanium trichloride ($TiCl_3$) was obtained from Pfalz and Bauer as a 30% wt/vol solution in 2.0 M HCl. All other chemicals were from Aldrich, Sigma, or Acros Organics (Morris Plains, NJ) and were of the highest purity. CoA biosynthetic enzymes (phosphopantetheine adenylyltransferase and dephospho-CoA kinase) from *Escherichia coli* were obtained by published methods (13). ¹H NMR was performed on a Varian INOVA 400 instrument.

Synthesis of Seleno-CoA. Seleno-CoA was obtained by means of a chemo-enzymatic synthetic strategy modified from published methods (14, 15). NMR spectroscopy was performed on each intermediate. Detailed methods are provided in *Synthesis of Seleno-CoA*, which is published as supporting information on the PNAS web site, www.pnas.org.

First, *Se*-benzylselenopantetheine was prepared by coupling

¶It is surprising that the Cu content was overlooked with such a well studied enzyme in which plasma emission analyses indicated that metals other than Ni and Fe were found at substoichiometric levels (19). Reexamining some early (*circa* 1983) plasma emission analyses corroborates that many preparations of CODH indeed lacked Cu; however, at that time, cells were cultured differently, the enzyme was isolated under different conditions, and the enzyme was not known to contain ACS activity. Therefore, a Cu-depleted enzyme with high CODH activity, but devoid of ACS activity, would not have been recognized. Once the *M. thermoacetica* CODH was recognized to be the ACS (22), preparations low in ACS were discarded without further analysis. Reexamining the results of metal analyses after 1987 and after the metal content had been ''established'' indeed reveals that Cu was present in variable amounts, similar to the amount observed in current enzyme preparations. Unfortunately, this Cu was overlooked because the focus of attention was on assessing integrity of each preparation by measuring the concentrations of the previously established metals. Another reason Cu was overlooked is that addition of Cu(II) to a solution containing CODH/ACS leads to inactivation (S.W.R., unpublished data).

sodium pantothenate to benzylselenoethylamine hydrobromide in the presence of hydroxybenzotriazole, *N*-ethylmorpholine, and 1-(3-dimethylaminopropyl)-3-ethyl carbodiimide in dimethylformamide. Next, *Se*-benzylselenopantetheine 4′-*O,O*-dibenzylphosphate was synthesized as described (14, 15) by phosphorylating *Se*-benzylselenopantetheine. Selenopantetheine 4′-phosphate was obtained by deprotecting the *Se*-benzylselenopantetheine 4′-*O,O*-dibenzylphosphate by treatment with sodium in liquid ammonia, dissolving in water, and adjusting the pH to neutrality by adding 1 M NaOH. To prepare seleno-CoA, 15 mM selenopantetheine 4′-phosphate, 35 mM ATP, 10 mM DTT, 10 mM MgCl$_2$, phosphopantetheine adenylyltransferase (62 μg), and dephospho-CoA kinase (86 μg) were reacted in 100 mM Tris·HCl buffer (pH 7.6). Reactions were initiated by addition of the biosynthetic enzymes, incubated for 3 h at 37°C, and stopped by heating at 95°C for 5 min, and the precipitated protein was removed by centrifugation (13,000 rpm for 5 min in an Eppendorf centrifuge). The diselenide product was purified by chromatography on a DEAE-cellulose column using a gradient of NH$_4$HCO$_3$ (50–800 mM) and monitoring the elution at 234 nm. The product eluted as the diselenide in the last fraction from the column at ≈500 mM NH$_4$HCO$_3$. The lyophilized dry product was stored. Reduction of the diselenide to seleno-CoA was performed by treatment with a 2-fold excess of sodium borohydride. Complete conversion to seleno-CoA was obtained, as determined with Ellman's reagent (16).

Purification and Manipulation of CODH/ACS. *Moorella thermoacetica* (formerly *Clostridium thermoaceticum,* strain ATCC 39073) was grown with glucose as the carbon source at 55°C in undefined (17) or defined (18) media. CODH/ACS was purified under strictly anaerobic conditions (19) in a Vacuum Atmospheres (Hawthorne, CA) anaerobic chamber maintained at 18°C at an oxygen tension below 1 ppm. Oxygen levels were monitored continuously with a model 317 trace oxygen analyzer (Teledyne Analytical Instruments, City of Industry, CA). CODH/ACS was >95% pure on the basis of denaturing SDS/PAGE. Purified CODH/ACS had an average specific activity of 600 units (U)/mg (1 U = 1 μmol of CO oxidized per min) at 55°C and pH 7.6 with 10 mM methyl viologen as electron acceptor (19). The average specific activity of CODH/ACS in the isotopic exchange reaction between CO and [1-^{14}C]acetyl-CoA was 0.16 U/mg at 55°C when 200 μM acetyl-CoA, 0.57 mM CO, 0.1 M Mes (pH 6.0), and 0.1 mM methyl viologen were used. Reactions were started by

adding radiolabeled acetyl-CoA. Protein concentrations were determined by the Rose Bengal method (20). Metal analysis was performed at the Chemical Analysis Laboratory at the University of Georgia (Athens, GA) by using inductively coupled argon plasma (ICP) detection for 20 elements.

Metal Removal. Ammonium tetrathiomolybdate (generously supplied by Dimitri Coucouvanis, University of Michigan, Ann Arbor) was dissolved in anaerobic water and used immediately because hydrolysis to trithiomolybdate, dithiomolybdate, and monothiomolybdate occurs over time. The sample was homogeneous on the basis of its UV–visible spectrum (the extinction coefficients at 467 and 317 nm are 1.24×10^4 and 1.76×10^4 M^{-1}·cm^{-1}, respectively). Before metal removal experiments, the protein samples were freed of DTT by several cycles of concentration and dilution in an Amicon stirred cell apparatus. This step has been found to be required for the removal of labile Ni from cluster A (8). Desalted CODH/ACS was treated with pure anaerobic nitrous oxide (N$_2$O) before addition of tetrathiomolybdate. At the end of the reactions, the chelators were removed from the protein samples by concentration and dilution into 0.1 M Tris·HCl (pH 7.60). Metal analysis and activity assays were performed on the desalted samples. The desalting buffer was used as a background control.

EPR and X-Ray Absorption Spectroscopy (XAS). X-band EPR spectra were recorded in a Bruker ESP300e spectrometer connected to a Hewlett–Packard Microwave Frequency Counter model 5253B and a Bruker Gaussmeter model ER 035.

XAS experiments were performed at beamline 9-3 at the Stanford Synchrotron Radiation Laboratory (SSRL) by using Si(220) monochromator crystals. The energy was calibrated by using metal foil as an internal standard in a three-ion chamber geometry. The first inflection point of the Ni, Zn, Cu, and Se foil spectra was calibrated to 8331.6, 8980.3, 9660.7, and 12658.0 eV, respectively. The beam was fully tuned by using a harmonic rejection mirror with an energy cut-off at 12 keV for Ni, Cu, and Zn edges and 15 keV for the Se edge. During all x-ray measurements, the samples were maintained at ≈10 K by using an Oxford Instruments CF1208 helium flow cryostat. The spectra were recorded up to $k = 13$ Å^{-1} for Ni and Cu extended x-ray absorption fine structure (EXAFS), and $k = 14$ Å^{-1} for Zn and Se EXAFS in 30-min scans (four to six scans per sample). The fluorescence data were collected by using a Canberra 30-element Ge detector

Table 1. Copper requirement for activity of CODH and ACS from *Moorella thermoacetica* and *Methanosarcina thermophila*

Sample	CODH activity, U/mg	Acetyl-CoA/CO exchange, mU/mg	NiFeC per heterodimer, spins per $\alpha\beta$	Metal atoms per heterodimer ($\alpha\beta$)			
				Cu	Fe	Ni	Zn
As isolated	600	160	0.24	0.96	13.3	2.3	0.06
Desalted	510	92	0.22	0.76	12.1	2.0	0.38
EDTA	340	28	0.06	1.12	12.0	1.9	0.40
Neocuproine	520	35	0.20	0.83	11.2	1.8	0.16
o-Phenanthroline	320	ND	0.01	0.90	11.0	1.6	0.24
Tetrathiomolybdate	100	23	0.04	0.25	12.0	2.0	0.46
M. thermophila complex	140	150*	0.13	0.63	16.3	2.2	0.74

Conditions: See text for methods of determining CODH and ACS activities. EPR spectra were recorded at 80 K, power = 40 mW, gain = 20,000, modulation frequency = 100 kHz, and modulation amplitude = 10 gauss. Standard errors in metal analysis are about <0.12 ppm, which corresponds to <0.1 metal per heterodimer. ND, not detected.
*Acetyl-CoA/CO exchange activity for the CODH complex from *M. thermophila* was measured in the presence of 0.98 mM titanium(III) citrate.

and Canberra 2026 amplifiers with 0.125-μsec shaping times. Co, Ni, Cu, or Ga filters (optical density = 6) were used for Ni, Cu, Zn, or Se edge, respectively, to absorb most of the elastic scattered photons. Single-channel analyzers were used to set electronic windows on the Ni, Cu, Zn, or Se Kα fluorescence. The signal count rate at each individual detector element was between 4,000 and 7,000 cps, while the total count rates were on the order of 70,000 cps at the end of each scan. XAS data were analyzed as described previously (21).

Results

The recent crystal structure of the *M. thermoacetica* CODH/ACS revealed that the A cluster in the ACS active site contains a [4Fe-4S] cluster bridged to a binuclear Cu–Ni site (4). That the presence of Cu could have eluded detection for so many years is surprising.¶ Thus, we used several approaches to determine whether copper is essential and, if so, to assess its role. We determined the amount of copper, nickel, iron, and zinc among various enzyme preparations obtained from cells grown in media lacking copper or containing 0.1–1 μM CuCl$_2$, and with reduced Zn concentrations. Concentrations of Cu higher than 1 μM in the medium have detrimental effects. For example, growth of *M. thermoacetica* in the presence of 10 μM Cu^{2+} results in a 50% decrease in the growth rate and an enzyme with 50% lower CODH and ACS activity and severely altered metal content (1.4 Cu, 8.0 Fe, 1.3 Ni, and 0.72 Zn per heterodimer). We also treated CODH/ACS with several copper chelators under various conditions. Bathocuproine and neocuproine remove both Ni and Cu from CODH/AVS, whereas *o*-phenanthroline is fairly selective for removing Ni and tetrathiomolybdate for depleting Cu (Table 1). This reagent can selectively remove Cu(I) from proteins, including metallothionein, and is used in anticopper therapies for Wilson's disease and metastatic cancer (23, 24).

Anecdotal information is available correlating ACS activity and NiFeC signal intensity. To establish a firm relationship (or lack thereof) between metal content and these activity measurements, we measured the metal content, the NiFeC signal intensity, and the ACS activity in a number of enzyme preparations. Fig. 1*A* shows a strong relationship between NiFeC signal intensity and ACS activity. However, the relationship is not strictly linear. Thus, we correlated metal content with both activity parameters.

Because loss of the labile Ni from ACS results in lowered ACS activity (8), it is important to determine the effect of Cu depletion in samples with a full complement of Ni. By treating CODH/ACS with tetrathiomolybdate and by studying various preparations of enzyme from bacteria grown under various conditions, a fairly wide variation in Zn and Cu content is obtained, whereas the Ni (2.0) and Fe (14.0) contents are more consistent (Table 1, Fig. 1*B*). Interestingly, the total Cu + Zn content reaches ≈1.0 per mole of α subunit. Correspondingly, because earlier Ni depletion studies had been performed without addressing effects on Cu, we determined the activities of samples replete with Cu, but with lowered Ni (Fig. 1*B*). In such samples, the amount of Cu or Ni in CODH/ACS correlates directly with the ACS activity (Fig. 1*B*), which in turn correlates directly with the NiFeC EPR signal intensity (Fig. 1*A*). On the other hand, the amount of Zn is inversely related to both ACS activity and NiFeC signal intensity. CODH/ACS preparations devoid of zinc have high CODH and ACS activity, whereas preparations high in Zn are correlated with low ACS activity, but are uncorrelated with CODH activity (Table 1). This finding suggests that Cu and Zn can compete for the bridging position between Fe and Ni in the A cluster, that active enzyme contains Cu in that site, and that replacement of Cu by Zn destroys ACS activity. The *Methanosarcina thermophila* CODH/ACS also con-
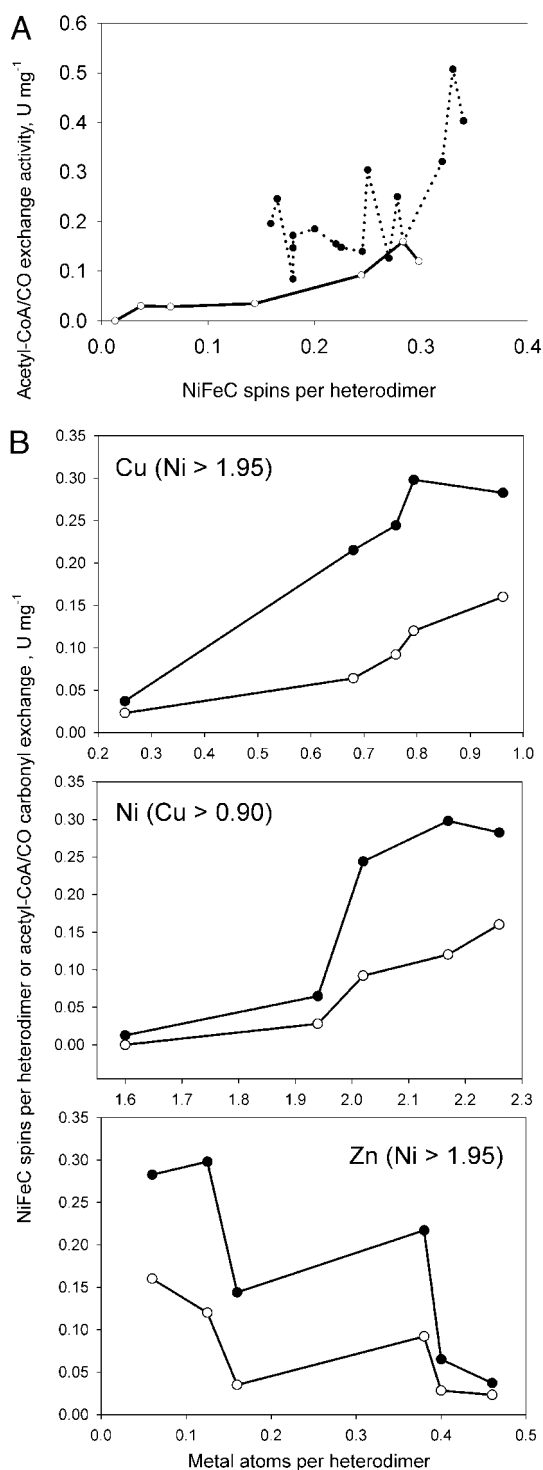

Fig. 1. Dependence of ACS activity and NiFeC signal intensity on metal content. (*A*) Dependence of the CO/[1-¹⁴C]acetyl-CoA exchange activity on the intensity of the NiFeC signal of CODH/ACS. ○, Data from Table 1; ●, data from 15 different as-isolated CODH/ACS preparations without chelator treatment. Exchange assays were monitored as described in *Materials and Methods*. Desalted ACS samples were treated with pure CO for 10 min before freezing and recording of the EPR spectra. The conditions for the EPR spectra were temperature, 77 K; power, 1–10 mW; gain, 20,000; modulation amplitude, 10 G; modulation frequency, 100 kHz. Spin concentrations were determined by double integrations of the EPR signal relative to a 1 mM Cu perchlorate standard. (*B*) Dependence of NiFeC signal intensity and the CO/[1-¹⁴C]acetyl-CoA exchange activity on the metal content of CODH/ACS from Table 1. ○, Exchange activity; ●, NiFeC signal intensity. The Cu and Ni dependencies correspond to samples with >1.95 Ni and >0.9 Cu per heterodimer, respectively.
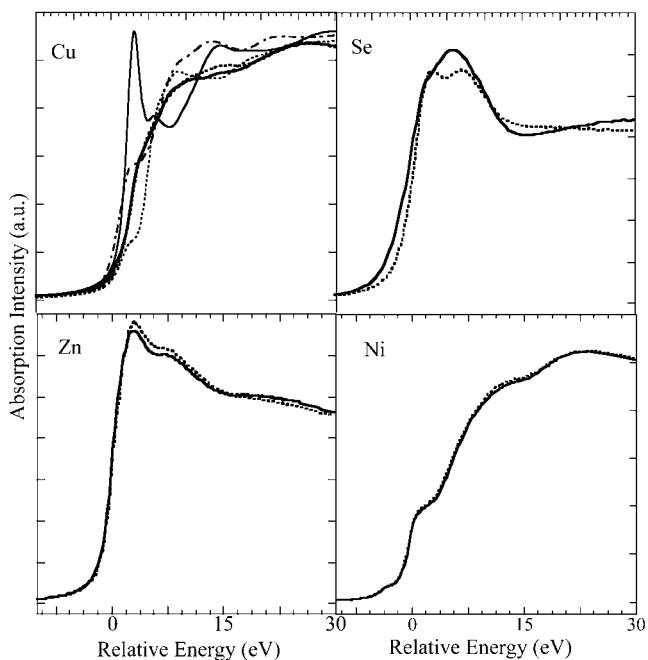
Fig. 2. Cu, Zn, and Ni x-ray absorption near-edge spectroscopy (XANES) of as-isolated (thick continuous line) and seleno-CoA-treated (dotted line) CODH/ACS; Se XANES of seleno-CoA in the absence (thick continuous line) and presence (dotted line) of enzyme. In the Cu panel, the Cu XANES of two-coordinate (thin continuous line) (26), three-coordinate (long-and-short-dashed line) (27), and four-coordinate (short-dashed line) (25) are compared with CODH/ACS. The energy at 0 eV is relative to 8,980, 9,663, 8,335, and 12,658 eV for Cu, Zn, Ni, and Se edges, respectively. a.u., Arbitrary units.

tains Cu (Table 1), suggesting that Cu may be a component of active ACS from all organisms.

Measurement of the Cu K-edge XAS of CODH/ACS reveals that the shape of the edge is intermediate between that reported
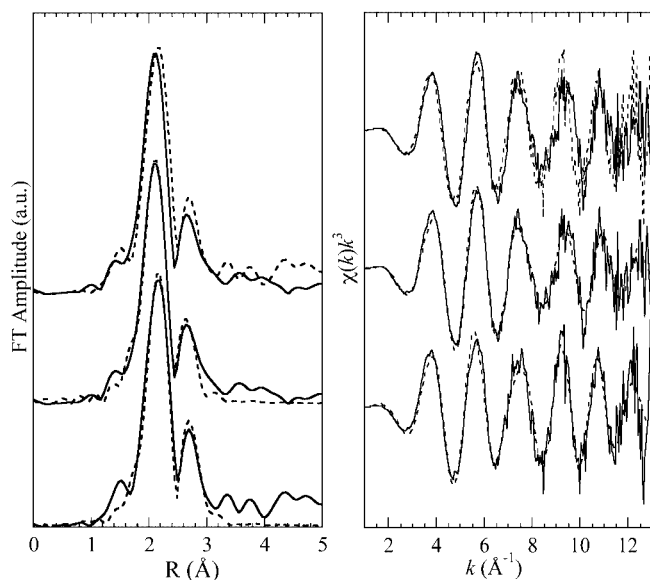
Table 2. Cu EXAFS fit parameters

Sample	Fit	N	R, Å	σ^2,* 10^3 Å	$F^†$
As isolated	1a	3 S	2.244	7.90	171.5
	2a	3 S	2.248	7.49	108.2
		1 Ni	2.646	8.82	
Se-CoA-treated	1a	3 S	2.270	6.90	252.5
	2a	3 S	2.280	6.90	186.1
		1 Ni	2.727	6.99	
	3a	3 S	2.249	8.66	166.4
		1 Ni	2.699	4.78	
		1 Se	2.437	7.74	

*σ^2 is the mean-square deviation of R.
†The goodness-of-fit parameter $F = \Sigma (\chi_{calc} - \chi_{obs})^2 k^6$.

for other Cu(I)S$_3$ and Cu(I)S$_4$ species (25–27), and it clearly rules out two-coordinate Cu(I) (Fig. 2). The inflection point energy of 8,983 eV is similar to the Cu(I) edge reported by Kau *et al.* (26) and Carr *et al.* (28) and is 6 eV lower than the inflection point for the Cu(II) form of blue copper proteins (29). Cu EXAFS spectra (Fig. 3) were first fit by including 3 S at 2.25 Å (Table 2). Adding one more S increases the Debye–Waller factor to an unreasonably high value. There is another dramatic feature at ≈2.6 Å in the Fourier-transformed (phase-shifted according to S) spectrum, which could be fit by a Cu–metal (Ni) interaction at 2.65 Å. The goodness-of-fit parameter improves significantly after adding the Cu–metal shell. The Cu–S and Cu–Ni distances obtained from the EXAFS fit are consistent with the crystal structure, which assigned three Cu–S bonds at distances ranging from 2.16 to 2.28 Å and a Cu–Ni bond distance of 2.69 Å. Therefore, XAS analysis of a freshly isolated and highly active form of ACS in solution agrees with x-ray crystallographic results that the A cluster of ACS contains a [4Fe-4S] cluster bridged to a binuclear Cu–Ni site.

In the proposed ACS reaction mechanism, a CoA thiolate performs nucleophilic attack on an acetyl-metal intermediate to release acetyl-CoA. The reactivity of thiol substrates is often enhanced by coordination to a metal center, which appears to present the active thiolate nucleophile to the electrophilic center (30). To test the hypothesis that the thiolate of CoA can ligate one of the metals in the A cluster, we performed XAS of CODH/ACS in the presence and absence of seleno-CoA. The Se edge and Se EXAFS in the presence and absence of CODH/ACS clearly demonstrate that seleno-CoA binds to a metal ion. The Se edge shifts by ≈1 eV to higher energy in the presence of CODH/ACS (Fig. 2), indicating a decrease in the effective anionic charge on the Se atom (31), which is consistent with Se binding to a metal center that acts as a Lewis acid. No noticeable change is observed in the Ni
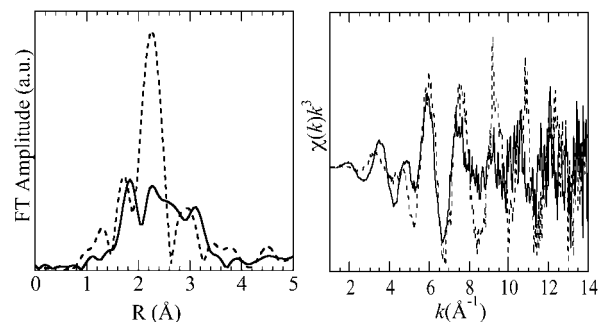

Fig. 3. (*Left*) Top traces, Fourier-transformed (FT) Cu EXAFS of CODH/ACS in the absence (continuous line) and presence (dashed line) of seleno-CoA. Middle and bottom traces, FT Cu EXAFS (continuous line) and best fit (dashed line) of as-isolated (middle) and seleno-CoA-treated (bottom) CODH/ACS. (*Right*) Cu EXAFS in *k* space with plotting symbols as described for *Left*.

Fig. 4. (*Left*) Fourier-transformed Se EXAFS of seleno-CoA in the absence (continuous line) and presence (dashed line) of CODH/ACS. (*Right*) Se EXAFS in *k* space with plotting symbols as described for *Left*.

edges of CODH/ACS, whereas minor modifications of the Cu and Zn edges occur in the presence of seleno-CoA (Fig. 2). Se EXAFS analysis (Fig. 4) indicates that the Se–metal distance is 2.39 Å. Consistent with the Se EXAFS, a metal–Se distance at 2.43 Å is found in Cu (Fig. 3) and Zn EXAFS (not shown); however, there is no indication of a Ni–Se interaction in the Ni EXAFS. XAS experiments of the enzyme in the presence of seleno-CoA reveal a Cu–S_3Se environment with a 2.43 Å Se-Cu bond, strongly implicating a Cu-SCoA intermediate in the mechanism of acetyl-CoA synthesis. XAS studies also indicate that Zn competes with Cu in CoA binding.

Although the S (or Se) group of CoA is expected to play a fairly minor role in the binding interactions, it is important to ensure that ACS binds CoASe(H?) similarly to CoASH. Because CoASH is a competitive inhibitor of the CO/acetyl-CoA exchange reaction, one can directly determine the binding constant for CoASH (as the K_i) from the inhibition kinetics. Seleno-CoA inhibited the exchange reaction between CO and [1-^{14}C]acetyl-CoA with an inhibition constant (K_i) of 213 ± 40 μM (see Fig. 6, which is published as supporting information on the PNAS web site), which is 30 times weaker than the natural sulfur–CoA ($K_i = 7$ μM) inhibitor, but 28 times stronger than desulfo-CoA ($K_i = 6$ mM), in which a hydrogen atom replaces the thiol group (32). These results suggest that the two molecules bind similarly and indicate a CoAS–Cu interaction, based on the Se and Cu XAS results.

Discussion

The CODH/ACS crystal structure reveals that the A cluster contains a Cu–S_3 center with three thiolate ligands. The Cu center forms a bridge between a square-planar Ni and one of the Fe sites in a [4Fe-4S] cluster. Here we have focused on the Cu center, which, before the crystal structure was determined, was not known to be a component of this enzyme. Here, we have shown that the amount of Cu in CODH/ACS directly correlates with ACS activity and with NiFeC EPR signal intensity. The metal-activity profiles shown in Fig. 1B indicate that Cu is not the only metal that can occupy the Cu site. Apparently, Cu is the metal of choice, because 1.0 mol of Cu per $\alpha\beta$ heterodimer is present in active enzyme isolated from cells grown in medium containing 1.0 μM Cu and 30 μM Zn. When Cu is not added to growth media containing 20 μM Zn, variable amounts of Zn and Cu are found, indicating that the trace amount of Cu present in the yeast extract, tryptone, and other medium components is scavenged and incorporated into the A cluster. The negative correlation between Zn content and ACS activity suggests that this metal can replace Cu and inhibit the enzyme.

A methanogenic CODH/ACS also contains near-stoichiometric amounts of copper, which is not surprising because the EPR spectra of the A clusters of the CODH/ACS from acetogens and methanogens are highly similar (33). Interestingly, an early description of the methanogenic *Methanosarcina barkeri* CODH reported stoichiometric amounts of copper (10); however, this was the CODH-only form of the enzyme lacking ACS. At least, based on the recent crystal structure of the *M. thermoacetica* CODH/ACS complex (4), there was no evidence for copper in the CODH component.

The results of XANES studies reveal that Cu(I) is present in the as-isolated enzyme. This is consistent with the absence of Cu(II) EPR signals from in any states of the enzyme so far studied. The Cu(II)/(I) redox couple must be very positive, because even N_2O-treated enzyme does not exhibit a Cu(II) EPR signal.

In the CODH/ACS crystal structure, the Cu(I) center contains four ligands, including three thiolates from cysteine residues 509, 595, and 597 and an extra ligand, perhaps an
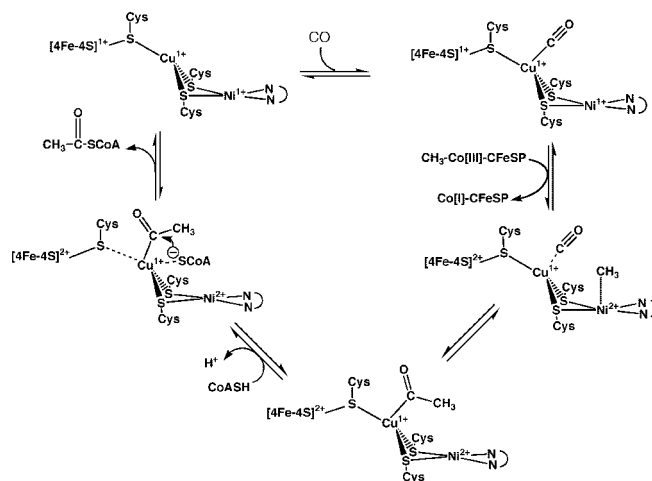

Fig. 5. Proposed mechanism of acetyl-CoA synthesis.

acetyl intermediate, in a distorted environment. The bond angles between the three Cu–S vectors in the crystal structure are 120°, 83°, and 140°, instead of the 109° expected for a tetrahedral site or 120° for a trigonal site. The XANES experiment also indicates that the Cu site is distorted with an x-ray absorption edge position midway between that of a trigonal and tetrahedral site, consistent with the crystal structure. On the basis of EXAFS experiments, the average Cu–S distance is 2.25 Å and the Cu–Ni distance is 2.65 Å, which is similar to that shown in the crystal structure (2.8 Å). Therefore, XAS results indicate that the active form of the A cluster of ACS contains a distorted Cu(I)–S_3 center with properties nearly identical to those measured in the crystal structure. Because the x-ray structure analysis was performed on crystals grown in high concentrations of acetate buffer, whereas the protein studied by XAS was in buffer lacking acetate, the minor differences between the two analyses may derive from the extra electron density at the Cu(I) site in the x-ray structure that was interpreted as an Cu-acetyl intermediate. EXAFS studies can be used to test the presence of a Cu–carbon bond in enzyme prepared under conditions identical to those in the crystallization, i.e., in the presence of 0.3 M acetate.

The Se and Cu EXAFS spectra of the seleno-CoA-incubated enzyme reveal a Cu–S_3Se environment with an $\approx$2.4-Å Se–Cu bond. These, combined with the seleno-CoA inhibition results, suggest that CoASH and CoASe bind similarly to ACS and indicate a CoAS–Cu interaction. The x-ray structure revealed a large cavity between the three domains that constitute the ACS subunit (4). CoA can be modeled into this region, which also contains Trp-418 and six Arg residues that have been implicated in CoA binding, on the basis of fluorescence and specific arginine modification studies (22, 34). Here we have obtained evidence for a Cu(I)–SCoA intermediate. Perhaps one role for Cu is to catalyze CoASH deprotonation, since the pK_a for the CoA thiol is 9.7 and the CoA thiolate would be required for nucleophilic attack on a bound acetyl intermediate. Many enzymes that use nucleophilic thiols contain a zinc ion that coordinates the thiol substrate, forming a thiolate at neutral pH; examples include methyltransferases such as methionine synthase, the adenosine deaminase DNA-repair protein, and farnesyl- and geranylgeranyl-protein transferases (30).

Fig. 5 is a proposed bioorganometallic mechanism of acetyl-CoA synthesis. The most solid information about which metal binds which substrate is the CoASe–Cu XAS data presented here. The crystal structure also provided evidence for

Cu–CO and acetyl-Cu intermediates (4). The first step, carbonylation of ACS, generates a paramagnetic species called the NiFeC species, whose intensity correlates with increased ACS activity (Fig. 1*A*). This species has been observed by Fourier transform IR (35) and EPR (36, 37) spectroscopy and shown to be a catalytically competent intermediate in the pathway (9). It is so named because nuclear hyperfine interactions are observed from enzyme with ^{61}Ni and ^{57}Fe, and from bound ^{13}CO (38, 39). The crystal structure shows the CO channel terminating at the Cu, indicating a Cu–CO (4), as shown in Fig. 5. It was assumed that the EPR signal results from a spin-coupled Ni^{1+}-X-[4Fe-4S]$^{2+}$ complex and that the hyperfine interactions result from exchange interactions between Ni^{1+} and an Fe site in the cubane (40). However, having a diamagnetic Cu(I) species bridging the Ni and the [4Fe-4S] cluster raises the possibility, as shown in Fig. 5, that the NiFeC EPR signal arises from strong dipolar interactions between a reduced [4Fe-4S]$^{1+}$ cluster and Ni^{1+}. This phenomenon would be similar to the radical doublet observed in some adenosylcobalamin-dependent reactions (41, 42). In these biradical systems, Co(II) and an organic radical intermediate exhibit strong enough dipolar coupling to observe nuclear hyperfine interactions from Co(II) and from the substrate protons/deuterons.

The next step in the reaction, methylation of ACS, has been suggested to occur at Ni because removal of "labile nickel" prevents methylation (43). It is clear that methylation converts the paramagnetic form of the A cluster to a diamagnetic state (9). Methylation of Ni(I) would generate a transient methyl–Ni(III) species, and, if the cluster is reduced, it could donate an electron to generate methyl–Ni(II) and [4Fe-4S]$^{2+}$. This would be a true diamagnetic and EPR-silent state, in accordance with rapid kinetics results. Migration of the methyl group to a Cu–CO would generate the acetylated enzyme, which, based on the crystal structure, could be an acetyl-Cu species (4). Here we have obtained evidence for a Cu(I)–SCoA intermediate and suggest that coordination of the sulfur to Cu stabilizes the active nucleophilic thiolate form of CoA to react with the acetyl intermediate and generate acetyl-CoA.

In summary, the combined kinetic and spectroscopic results indicate an essential and functional role for copper in the A cluster of CODH/ACS.

1. Ragsdale, S. W. (2000) in *Enzyme-Catalyzed Electron and Radical Transfer*, eds. Holzenburg, A. & Scrutton, N. (Plenum, New York), Vol. 35, pp. 487–518.
2. Ragsdale, S. W. & Kumar, M. (1996) *Chem. Rev.* **96,** 2515–2539.
3. Ragsdale, S. W. (1999) in *Chemistry and Biochemistry of B₁₂*, ed. Banerjee, R. (Wiley, New York), Vol. 1, pp. 633–654.
4. Doukov, T. I., Iverson, T., Seravalli, J., Ragsdale, S. W. & Drennan, C. L. (2002) *Science* **298,** 567–572.
5. Diekert, G. B., Graf, E. G. & Thauer, R. K. (1979) *Arch. Microbiol.* **122,** 117–120.
6. Diekert, G. & Thauer, R. K. (1980) *FEMS Microbiol. Lett.* **7,** 187–189.
7. Ensign, S. A., Bonam, D. & Ludden, P. W. (1989) *Biochemistry* **28,** 4968–4973.
8. Shin, W., Anderson, M. E. & Lindahl, P. A. (1993) *J. Am. Chem. Soc.* **115,** 5522–5526.
9. Seravalli, J., Kumar, M. & Ragsdale, S. W. (2002) *Biochemistry* **41,** 1807–1819.
10. Krzycki, J. A., Mortenson, L. E. & Prince, R. C. (1989) *J. Biol. Chem.* **264,** 7217–7221.
11. Dobbek, H., Svetlitchnyi, V., Gremer, L., Huber, R. & Meyer, O. (2001) *Science* **293,** 1281–1285.
12. Drennan, C. L., Heo, J., Sintchak, M. D., Schreiter, E. & Ludden, P. W. (2001) *Proc. Natl. Acad. Sci. USA* **98,** 11973–11978.
13. Strauss, E. & Begley, T. P. (2002) *J. Biol. Chem.* **277,** 48205–48209.
14. Moffatt, J. G. & Khorana, H. G. (1961) *J. Am. Chem. Soc.* **83,** 663–675.
15. Gunther, W. H. H. & Mautner, H. G. (1965) *J. Am. Chem. Soc.* **87,** 2708–2716.
16. Ellman, G. L. (1958) *Arch. Biochem. Biophys.* **74,** 443–450.
17. Andreesen, J. R., Schaupp, A., Neurater, C., Brown, A. & Ljungdahl, L. G. (1973) *J. Bacteriol.* **114,** 743–751.
18. Lundie, L. L., Jr., & Drake, H. L. (1984) *J. Bacteriol.* **159,** 700–703.
19. Ragsdale, S. W., Clark, J. E., Ljungdahl, L. G., Lundie, L. L. & Drake, H. L. (1983) *J. Biol. Chem.* **258,** 2364–2369.
20. Elliott, J. I. & Brewer, J. M. (1978) *Arch. Biochem. Biophys.* **190,** 351–357.
21. Gu, W. W., Jacquamet, L., Patil, D. S., Wang, H.-X., Evans, D. J., Smith, M. C., Millar, M., Koch, S., Eichhorn, D. M., Latimer, M. & Cramer, S. P. (2003) *J. Inorg. Biochem.* **93,** 41–51.
22. Ragsdale, S. W. & Wood, H. G. (1985) *J. Biol. Chem.* **260,** 3970–3977.
23. Dabrio, M., Rodríguez, A. R., Bordin, G., Bebianno, M. J., Ley, M. D., Sestáková, I., Vasák, M. & Nordberg, M. (2002) *J. Inorg. Biochem.* **88,** 123–134.
24. Brewer, G. J., Dick, R. D., Grover, D. K., LeClaire, V., Tseng, M., Wicha, M., Pienta, K., Redman, B. G., Jahan, T., Sondak, V. K., *et al.* (2000) *Clin. Cancer Res.* **6,** 1–10.
25. George, G. N., Pickering, I. J., Yu, E. Y., Prince, R. C., Bursakov, S. A., Gavel, O. Y., Moura, I. & Moura, J. J. G. (2000) *J. Am. Chem. Soc.* **122,** 8321–8322.
26. Kau, L. S., Spira-Solomon, D. J., Penner-Hahn, J. E., Hodgson, K. O. & Solomon, E. I. (1987) *J. Am. Chem. Soc.* **109,** 6433–6442.
27. Pickering, I. J., George, G. N., Dameron, C. T., Kurz, B., Winge, D. R. & Dance, I. G. (1993) *J. Am. Chem. Soc.* **115,** 9498–9505.
28. Carr, H. S., George, G. N. & Winge, D. R. (2002) *J. Biol. Chem.* **277,** 31237–31242.
29. Shadle, S. E., Pennerhahn, J. E., Schugar, H. J., Hedman, B., Hodgson, K. O. & Solomon, E. I. (1993) *J. Am. Chem. Soc.* **115,** 767–776.
30. Matthews, R. G. & Goulding, C. W. (1997) *Curr. Opin. Chem. Biol.* **1,** 332–339.
31. Peariso, K., Zhou, Z. S., Smith, A. E., Matthews, R. G. & Penner-Hahn, J. E. (2001) *Biochemistry* **40,** 987–993.
32. Raybuck, S. A., Bastian, N. R., Orne-Johnson, W. H. & Walsh, C. T. (1988) *Biochemistry* **27,** 7698–7702.
33. Lu, W.-P., Jablonski, P. E., Rasche, M., Ferry, J. G. & Ragsdale, S. W. (1994) *J. Biol. Chem.* **269,** 9736–9742.
34. Shanmugasundaram, T., Kumar, G. K. & Wood, H. G. (1988) *Biochemistry* **27,** 6499–6503.
35. Kumar, M. & Ragsdale, S. W. (1992) *J. Am. Chem. Soc.* **114,** 8713–8715.
36. Ragsdale, S. W., Ljungdahl, L. G. & DerVartanian, D. V. (1982) *Biochem. Biophys. Res. Commun.* **108,** 658–663.
37. Ragsdale, S. W., Ljungdahl, L. G. & DerVartanian, D. V. (1983) *Biochem. Biophys. Res. Commun.* **115,** 658–665.
38. Ragsdale, S. W., Wood, H. G. & Antholine, W. E. (1985) *Proc. Natl. Acad. Sci. USA* **82,** 6811–6814.
39. Fan, C., Gorst, C. M., Ragsdale, S. W. & Hoffman, B. M. (1991) *Biochemistry* **30,** 431–435.
40. Xia, J. Q., Hu, Z. G., Popescu, C. V., Lindahl, P. A. & Munck, E. (1997) *J. Am. Chem. Soc.* **119,** 8301–8312.
41. Banerjee, R. & Ragsdale, S. W. (2003) *Annu. Rev. Biochem.*, in press.
42. Licht, S., Gerfen, G. J. & Stubbe, J. A. (1996) *Science* **271,** 477–481.
43. Barondeau, D. P. & Lindahl, P. A. (1997) *J. Am. Chem. Soc.* **119,** 3959–3970.